33rd EPS Conference on Plasma Phys. Rome, 19 - 23 June 2006 ECA Vol.**30I**, P-2.123 (2006)

Gyrofluid Turbulence Modeling of the Linear VINETA Device

G.N.Kervalishvili[1], R.Kleiber[1], R.Schneider[1], B.D.Scott[2], O.Grulke[1], T.Windisch[1]

Max-Planck-Institut für Plasmaphysik, EURATOM Association,

[1] *Wendelsteinstraße 1, D-17491 Greifswald, Germany*

[2] *Boltzmannstraße 2, D-85748 Garching, Germany*

I. Introduction

Active control and detailed studies of turbulence is one of the major research topics in fusion plasmas. Recent experiments show the importance of coherent high plasma density structures, so-called "blobs", in tokamak scrape-off-layer (SOL). These experiments indicate that in fusion devices significant part of cross-field transport in the SOL is carried by blobs [1]. It was shown that blobs also can exist in devices with linear magnetic geometry [2-4]. From experiments in the linear PISCES [2] device radial movement of blobs was reported. For devices with linear magnetic geometry no toroidal curvature exists and the radial movement in PISCES was explained by the concept of the neutral wind [5]. The formation and propagation of turbulent structures were also observed in the linear VINETA device [3,4]. In order to obtain a better understanding of formation and propagation of these structures in VINETA the three-dimensional gyrofluid code GEM3 for flux tube geometry [6] is used. In order to compare results of the simulations and experiments some modifications of GEM3 are necessary. The proper metrics for the cylindrical geometry is implemented, in the parallel direction sheath boundary conditions are used, radial dependency of the collisional frequency is taken into account, and neutrals are modeled using the concept of the neutral wind [5]. Computations are done for two different experimental scenarios, one with and one without annulus limiter [4,7].

II. Description of the Model

For the global simulations of the linear device VINETA the two-moment (density and parallel velocity) gyrofluid equations for electrons and ions are used. The original code has been modified for the geometry of a cylindrical annulus (r,θ,z). We consider the electrostatic case. The corresponding particle and momentum conservation equations (in suitable normalized units [6]) in gyrofluid formulation are given as follows:

$$\frac{\partial \tilde{n}_e}{\partial t} + (v_E \cdot \bigtriangledown)(n_0 + \tilde{n}_e) = -\bigtriangledown_\parallel \tilde{v}_\parallel, \tag{1}$$

$$-\hat{\mu}\frac{\partial \tilde{v}_\parallel}{\partial t} - \hat{\mu}(v_E \cdot \bigtriangledown)\tilde{v}_\parallel = -\bigtriangledown_\parallel\left(\tilde{\phi} - \tilde{n}_e\right) - 0.51\hat{\mu}\hat{v}_e n_0 \tilde{J}_\parallel. \tag{2}$$

for the electrons,

$$\frac{\partial \tilde{n}_i}{\partial t} + (u_E \cdot \bigtriangledown)(n_0 + \tilde{n}_i) + W_N \frac{1}{r}\frac{\partial \tilde{n}_i}{\partial \theta} = -\bigtriangledown_\parallel \tilde{u}_\parallel, \tag{3}$$

$$\hat{\varepsilon}\frac{\partial \tilde{u}_\parallel}{\partial t} + \hat{\varepsilon}(u_E \cdot \bigtriangledown)\tilde{u}_\parallel = -\bigtriangledown_\parallel\left(\tilde{\phi}_G + \tau_i \tilde{n}_i\right) - 0.51\hat{\mu}\hat{v}_e n_0 \tilde{J}_\parallel. \tag{4}$$

for the ions. Here, $\hat{\varepsilon} = \left(L_{\parallel}/L_{\perp}\right)^2$ and $\hat{\mu} = (m_e/M_i)\,\hat{\varepsilon}$, where $L_{\parallel}$ and $L_{\perp}$ are parallel and perpendicular scale length of the system, respectively. $\tilde{n}_{i,e}$, $\tilde{u}_{\parallel}$, , $\tilde{v}_{\parallel}$ represent the ion and electron density and velocity fluctuations, n_0 is the radially varying background density. $\tilde{J}_{\parallel} = \tilde{u}_{\parallel} - \tilde{v}_{\parallel}$ is the current and $\hat{\nu}_e$ is the normalized collisional frequency. In Eq.(3) the third term on the left hand side is due to the force density W_N caused by the neutral wind, where $(T_e/L_{\perp})W_N = \mu_{Ni}(NV)_{fast}(K_{fast} - K_{slow})$ [5], here μ_{Ni} is the reduced ion-neutral mass, $(NV)_{fast}$ is the flux of fast neutrals, and $K_{fast}(K_{slow})$ are the neutral-ion collision rate constant of fast (slow) neutrals.

Ions and electrons are coupled by the polarization equation:

$$\Gamma_1 \tilde{n}_i + \frac{\Gamma_0 - 1}{\tau_i}\tilde{\phi} = \tilde{n}_e, \tag{5}$$

where $\tau_i = T_i/T_e$ and $\tilde{\phi}$ is the potential which acts on the electrons (their gyroradius is neglected). The operators $v_E \cdot \bigtriangledown$, $\bigtriangledown_{\parallel}$, Γ_0 and Γ_1 are defined as follows:

$$v_E \cdot \bigtriangledown = \frac{1}{r}\left(\frac{\partial\tilde{\phi}}{\partial r}\frac{\partial}{\partial\theta} - \frac{\partial\tilde{\phi}}{\partial\theta}\frac{\partial}{\partial r}\right),\ \ \bigtriangledown_{\parallel} = \frac{\partial}{\partial z},\ \ \Gamma_0 = \left(1 - \rho_s^2\bigtriangledown_{\perp}^2\right)^{-1},\ \ \Gamma_1 = \left(1 - \frac{1}{2}\rho_i^2\bigtriangledown_{\perp}^2\right)^{-1}. \tag{6}$$

Here, ρ_s, ρ_i are the drift scale and ion gyroradius.

In the code the following boundary conditions are used: the radial boundary condition for the potential is modified at the inner boundary, for the $m = 0$ mode number and $m \neq 0$ mode numbers Neumann and Dirichlet boundary conditions are used, respectively. For all other variables in the r-direction values are set to zero at the boundaries. These boundary conditions are more suited for the center of the cylinder. The θ direction is periodic. For the z-direction open-field boundary conditions are used:

$$\tilde{u}_{\parallel}|_{z=\pm 0.5} = \pm\Gamma_D(\tilde{n}_e), \quad \tilde{v}_{\parallel}|_{z=\pm 0.5} = \pm\left[\tilde{u}_{\parallel} - \Gamma_D(\tilde{\phi} - \Lambda\tilde{n}_e)\right]|_{z=\pm 0.5}, \tag{7}$$

where $\Gamma_D = \hat{\varepsilon}^{-1/2}$ and $\Lambda = 2.037$. For all other variables derivatives are set to zero at the boundaries (for more details see Ref.[8]).

The details of the numerical implementation and normalization of these equations follow the original GEM3 code (see Ref. [6]).

III. Results

For the simulations presented here we use density profiles (Fig. 1) corresponding to two different experimental scenarios: one without and one with annulus limiter, which is used to increase the density gradient.

Experimental results for the first scenario are shown in figure 2, where time traces of normalized electron density fluctuations at three different radial positions with respect to the background density profile are plotted. The positions correspond to the radial gradient (A1), edge (B1) and far-edge (C1) regions, respectively (see Fig. 1). The plasma density fluctuations exhibit a different character across the radial plasma density profile as we can see from figure 2. In the density gradient region coherent density fluctuations can be observed (Fig. 2 top). In the plasma edge density fluctuations exhibit intermittent character, where the amplitude of the positive density bursts is twice higher than for the negative ones (Fig. 2 middle). The intermittent character of density fluctuations further increases in the far-edge region, where the background density is very low (Fig. 2 bottom).

A similar picture can be observed from the simulations for the first (Fig. 3) and second (Fig. 4) profile, where the density fluctuations are also plotted for the three different radial positions with respect to background density profile. The simulation domain is defined as $r \in [0.6\rho_s, 10\rho_s]$, $\theta \in [-\pi, \pi]$, $z \in \left[-0.5L_{\|}, 0.5L_{\|}\right]$, where $L_{\|} = 451.2\ cm$ is the system length and the number of grid points is $32 \times 128 \times 16$ in $\{r, \theta, z\}$. As we can see from figures 3 and 4 (bottom) in the far-edge region (C1, C2) the intermittent density fluctuations are characterized by the same order of magnitude as in the gradient region (A1, A2). In the case of the second profile, with higher background density gradient, in the regions of edge (B2) and far edge (C2) the character of bursts are more pronounced (Fig. 4 middle and bottom).

For the first profile in the saturated turbulence phase simulations are also done for two different values of the W_N parameter (Fig. 5 and 6) in order to exhibit the influence of the neutral wind on the radial plasma motion. A very crude estimate of the W_N parameter is using the maximum possible parameters for VINETA: the value of K_{slow} is assumed to be zero and for K_{fast} and V_{fast} sound velocities are used with the maximum value of the ion temperature. As we can see from figure 5 the behaviour of fluctuations are the same for all the three regions and exhibits strong intermittent character in contradiction to the experimental observation in the gradient region. Plots for a more realistic W_N parameter (reduced by a factor of 10 compared with the maximum value) are shown in figure 6. The influence of the neutral wind is not so strong. The character of the fluctuations in all three regions are more similar to those where $W_N = 0$ (Fig. 3) with more pronounce intermittent structures outside the gradient region.

IV. Conclusions

We have modified the original GEM3 code for cylindrical annulus geometry in order to use it for the simulation of the linear device VINETA. The modified code gives us similar results as observed in experiments. The influence of the neutral wind was studied qualitatively, but full quantitatively comparison still needs to be done.

References

[1] S.I. Krasheninnikov, Phys. Lett. A **283**, 368 (2001).

[2] G.Y. Antar et al, Phys. Plasmas **10**, 419 (2003).

[3] T. Windisch, O. Grulke, T. Klinger, accepted for publication in Phys. Scripta 2005.

[4] O. Grulke, T. Windisch, T. Klinger, paper at PSI conference 2006.

[5] S.I. Krasheninnikov, A.I. Smolykov, POP **10**, 3020 (2003).

[6] B.D. Scott, Plasma Phys. Contr. Fusion **45**, A385 (2003).

[7] T. Windisch et al, paper at EPS conference 2006.

[8] T.T. Ribeiro, B.D. Scott, Plasma Phys. Contr. Fusion **47**, 1657 (2005).

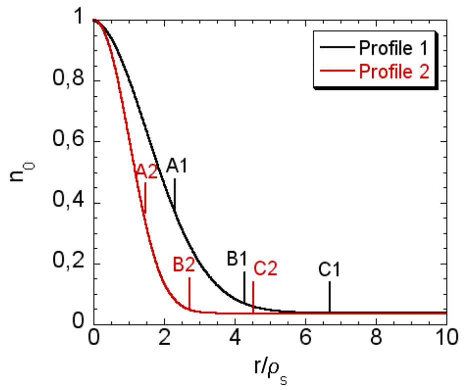

Figure 1: Normalized background density profiles.

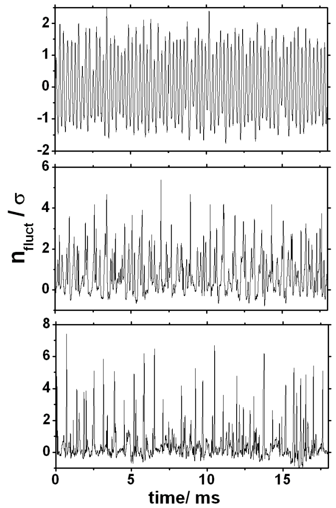

Figure 2: Electron density fluctuations (Experiment, first scenario).

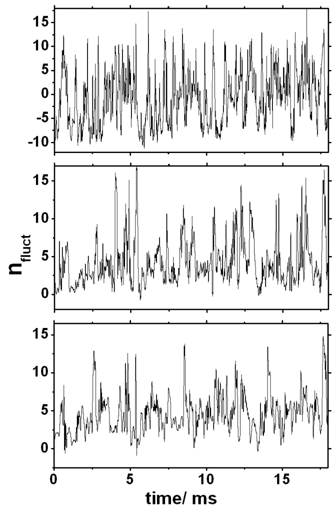

Figure 3: Normalized electron density fluctuations (Simulation, first profile).

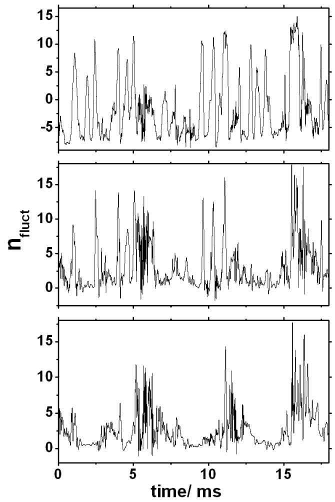

Figure 4: Normalized electron density fluctuations (Simulation, second profile).

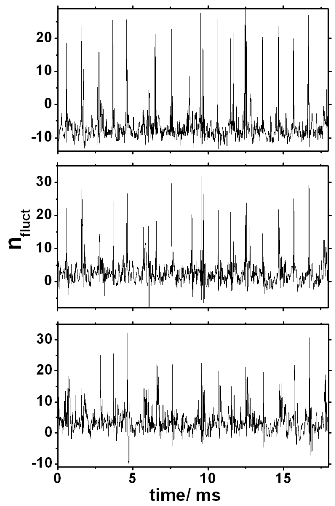

Figure 5: Normalized electron density fluctuations $W_N = 1.820$ (Simulation, first profile).

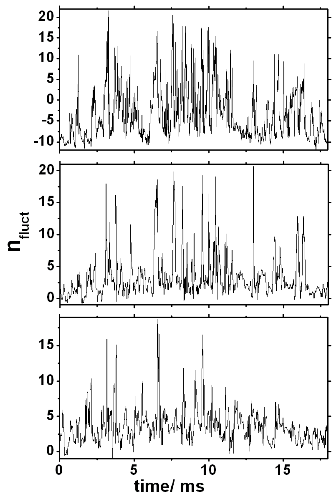

Figure 6: Normalized electron density fluctuations $W_N = 0.182$ (Simulation, first profile).